Calibration experiments of ^{3}He neutron detectors for analyzing neutron emissivity in the hot-ion mode on the GAMMA 10 tandem mirror

J. Kohagura,[a] T. Cho, M. Hirata, H. Watanabe, R. Minami, T. Numakura, M. Yoshida, H. Ito, Y. Tatematsu, K. Yatsu, and S. Miyoshi
Plasma Research Centre, University of Tsukuba, Ibaraki 305-8577, Japan

K. Ogura
Niigata University, Niigata 950-2181, Japan

T. Kondoh and T. Nishitani
Japan Atomic Energy Research Institute, Ibaraki 319-1195, Japan

M. Kwon and A. C. England
National Fusion R&D Center, Korea Basic Science Institute, Daejeon, Republic of Korea

(Presented on 9 July 2002)

Under the international fusion cooperating research, ^{3}He neutron detectors in the GAMMA 10 tandem mirror are calibrated by the use of a ^{252}Cf spontaneous fission neutron source (8.96×10^4 n/s). The calibration experiments are carried out with a ''rail system'' placed along the magnetic axis of the GAMMA 10 central-cell region, where hot ions in the plasma experiments with the bulk temperatures of ~10 keV are produced. As compared to a previous neutron monitoring system with a BF_3 detector in GAMMA 10, the present ^{3}He systems are designed with about two orders-of-magnitude higher neutron-counting efficiency for analyzing a neutron emissivity from the plasmas in a single plasma discharge alone. Two ^{3}He systems are installed near the middle and the end of the central cell so as to identify the central-cell hot-ion axial profile. The filling pressure of ^{3}He, the effective length, and the diameter of the detector are designed as 5 bar, 300 mm, and 50 mm, respectively. The detector output spectra are carefully analyzed by the use of a preamplifier, a shaping amplifier, as well as a multichannel analyzer for each ^{3}He detector. In the present article, the neutron-counting data from the two ^{3}He detectors due to the on-axis ^{252}Cf scan are interpreted in terms of the d^{-2} intensity dependence (d being the distance between the detector and the neutron source) as well as the effects of the central-cell magnetic coils and the other machine structural components. [DOI: 10.1063/1.1534402]

I. INTRODUCTION

One of the representative operational modes in GAMMA 10[1–5] is characterized in terms of a hot-ion mode[6,7] with bulk-ion temperatures T_i of 10–20 keV by the use of ion-cyclotron heatings (ICHs).[8] In the recent fundamental hot-ion-mode experiments with deuterium-proton mixed plasmas having $T_i \approx 10$ keV, it is reported that the count rate of neutrons produced by deuterium-deuterium (D-D) reactions is observed to increase with increasing the bulk-ion diamagnetisms.[6] Also, a high-potential operational mode[1,5,9] having kV-order plasma-confining potentials has been investigated in GAMMA 10. A large part of the database obtained from these two operations has intensively been investigated and summarized by using a proposal[2–4] of combining the two major theories, i.e., Cohen's strong electron-cyclotron heating theory[10] and the generalized Pastukhov potential-confinement theory,[11,12] so as to highlight the common essential physics bases underlying these modes and to achieve upgraded operational modes having hot-ion plasmas with high potentials in future experiments. Verification of the effectiveness of potential confinement on improving the plasma parameters of the tandem-mirror plasmas in the hot-ion mode experiments with D-D reactions is of great importance for the future tandem-mirror physics researches.

In the present article, in order to investigate the potential-confinement effects on improvements in the D-D fusion reaction rate, ^{3}He systems are calibrated by the use of a ^{252}Cf neutron source. For the ^{3}He systems, improved neutron-detection efficiencies of the two orders-of-magnitude higher than those for the previously installed neutron monitoring system with a BF_3 detector[6] are demonstrated. The advantageous high-count rate provides an efficient quick survey for finding an optimized plasma operational regime along with the information on plasma-parameter dependence from the viewpoint of a high neutron-count rate by the use of a limited number of the plasma discharges.

II. EXPERIMENTAL APPARATUS

A. GAMMA 10 tandem mirror

GAMMA 10[1–4] is a minimum-B anchored tandem mirror with an outboard axisymmetric plug and barrier cells. It has an axial length of 27 m, and the total volume of the

[a]Electronic mail: kohagura@prc.tsukuba.ac.jp

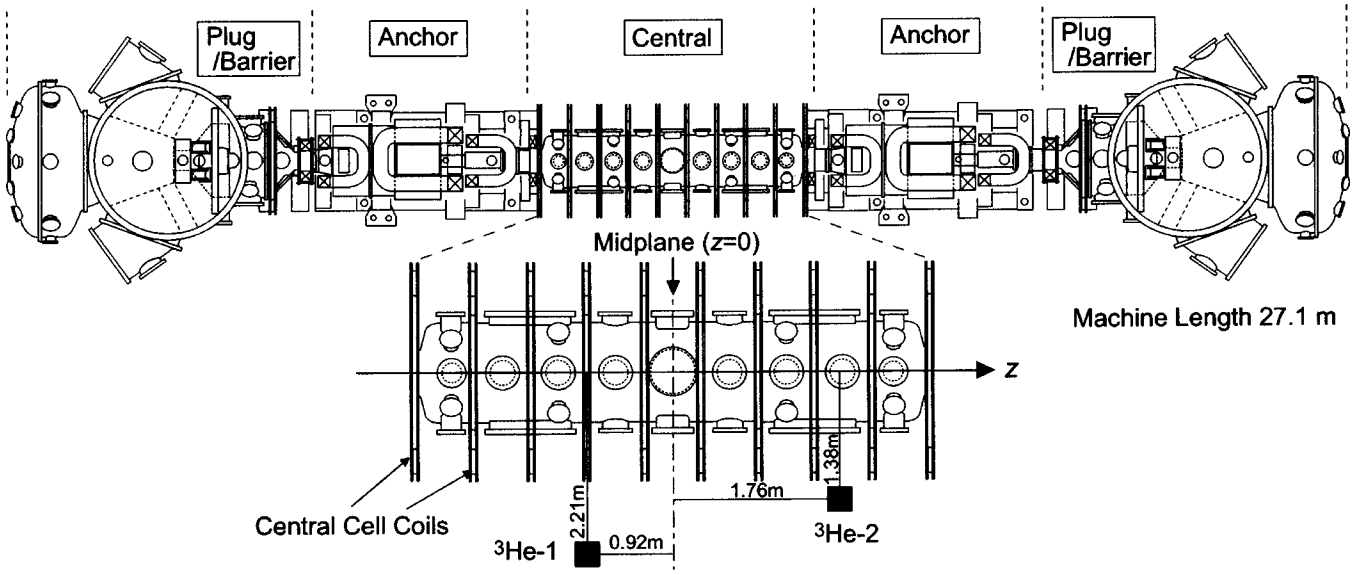

FIG. 1. A top view of the GAMMA 10 tandem mirror along with the expanded schematic drawings of the central cell including the geometrical configurations of two ^{3}He detectors. These ^{3}He detectors locate at $z=-0.92$ m and $r=2.21$ m, as well as $z=1.76$ m and $r=1.38$ m, respectively. Here, the location of the central-cell midplane is defined as $z=0$, and the distance of the detector from the magnetic axis ($r=0$) is designated as r.

vacuum vessel is 150 m^3. The central cell has a length of 6 m and a fixed limiter with a radius of 0.18 m.

The main tandem-mirror operations in GAMMA 10 are characterized in terms of (a) a high-potential mode having kilovolt order plasma confining potentials[1–5] and (b) a hot-ion mode yielding D-D fusion produced neutrons with 10–20 keV bulk-ion temperatures.[6,7] When hot-ion-mode experiments with a deuterium-proton mixed plasma are carried out, the deuterium ions added to protons by gas puffing are heated by means of the slow wave absorptions in the ion cyclotron range of frequency (ICRF)[8] at 4.465 MHz having the fundamental resonance in the central cell, while the protons are heated by ICRF fast waves at 9.9 MHz in the minimum-B anchors in order to sustain magnetohydrodynamics stability of the whole plasma. The plug and barrier cells are axisymmetric mirrors with an axial length of 2.5 m adjacent to the anchor cells. Microwaves (150 kW at 28 GHz) are injected in the extraordinary mode into the plug and the barrier regions to produce an ion-confining potential ϕ_c, and a thermal-barrier potential ϕ_b, respectively.

B. Calibration of ^{3}He neutron detectors

Schematic drawings of the locations of two ^{3}He systems on the GAMMA 10 tandem mirror are shown in Fig. 1. Here, the z-axis is designated in the direction along the magnetic axis of the central-cell solenoids with the origin ($z=0$) at the central-cell midplane. The ^{3}He detectors labeled ^{3}He-1 and ^{3}He-2 are installed near the middle ($z=-0.92$ m, and the radial distance from the magnetic axis $r=2.21$ m) and the end of the central cell ($z=1.76$ m, $r=1.38$ m), respectively.

Schematic drawings of the cylindrical moderated ^{3}He proportional counters[13,14] (Eurisys Measures: 133NH30/5) with a 50-mm-thick paraffin are employed as shown in Fig. 2(a). The paraffin moderator is covered over a 1-mm-thick Cd shield in order to absorb thermal neutrons moderated in

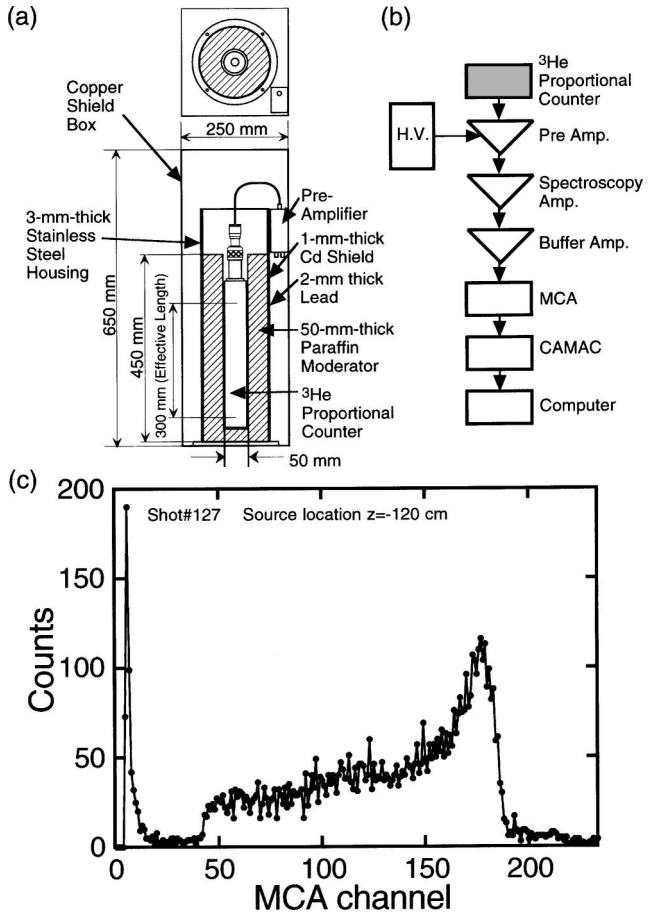

FIG. 2. Schematic drawings of (a) the ^{3}He proportional counters surrounded by a 50-mm-thick paraffin moderator, a 1-mm-thick Cd sheet, and a 2-mm-thick lead shield, and (b) a block diagram of the electronics employed for the data acquisition. (c) The pulse-height spectrum from ^{3}He-1 for a dwelling time of 576 s with the source position at $z=-1.20$ m inside the vacuum vessel. The spectrum shows a typical continuous pulse-height distribution which includes "wall effects" of ^{3}He proportional counters.

nearby structures. The diameter and the effective length of the ^{3}He proportional counter having 5-bar filling pressure are 50 and 300 mm, respectively.

Figure 2(b) shows the schematic block diagram of the electronics used for the neutron data acquisition. An output signal from the detector is connected to a preamplifier, a shaping amplifier, a buffer amplifier, and a multichannel pulse-height analyzer (MCA). The detector and the preamplifier are shielded against ICRF noises by a 1.5-mm-thick copper box [see Fig. 2(a)]. The set of a high-voltage power supply, a shaping amplifier, and a buffer amplifier is contained in a copper shield box as well, which is placed near the detector system.

The calibration experiments are carried out by using a ^{252}Cf neutron source (Amersham International plc.). The ^{252}Cf source yields neutrons by spontaneous fission reaction; the energy distribution of neutrons can be written by the use of a Maxwellian distribution which has the mean energy of 2.14 MeV with the residual nuclear temperature of 1.42 MeV.[13–15] The calculated source strength during the experiment is 8.96×10^4 n/s. The neutron source is moved along a thin aluminum rail placed on the magnetic axis ($r_c=0$) inside the GAMMA 10 vacuum vessel. The calibration experiments are made with a dwelling time of 576 s at each location from $z=1.80$ m to $z=-1.80$ m at intervals of 0.15 m.

III. CALIBRATION RESULTS

A. On-axis ^{252}Cf scan

Figure 2(c) shows the output spectrum obtained from ^{3}He-1 for 576 s with the neutron-source location at $z=-1.20$ m inside the GAMMA 10 vacuum vessel. Neutrons are detected in the ^{3}He proportional counters by means of the ^{3}He$(n,p)T$ reactions with the reaction energy of 765 keV which is shared between a proton (574 keV) and a triton (191 keV). As the ranges of a proton and a triton in the 5-bar ^{3}He counter have lengths of the order of one centimeter or less,[16] protons and/or tritons produced by reactions occurring near the detector wall can reach the wall and lose some energies to the wall. Such events (hereafter referred to as wall effects[15,16]) produce signal pulses smaller than those from events in which the whole reaction energy is absorbed by ^{3}He gas. Such wall effects can be seen in Fig. 2(c) as a continuous pulse-height distribution starting from ~40 MCA channel (~191 keV) to the ^{3}He$(n,p)T$ change of slope at ~160 MCA channel energy (~690 keV).

In Fig. 3(a), the data points represent the variation of the output-signal counts obtained from ^{3}He-1 during a 576-s dwelling time with the ^{252}Cf source position on the z-axis. Here, the hatched area labeled (A) represents the source locations, where the lines of sight of the ^{3}He detector cross the locations of the GAMMA 10 magnetic pancake coils and the coil supporting steel structures. The hatched area (B) in Fig. 3(a) represents the source positions, where a steel casing covering over a magnetic coil alone crosses the lines of sight. Here, the separated distance between the neighboring magnetic coils is 0.60 m. A characteristic oscillatory structure of the neutron counts in Fig. 3(a) results mainly from the existence of the periodically placed magnetic coils and the

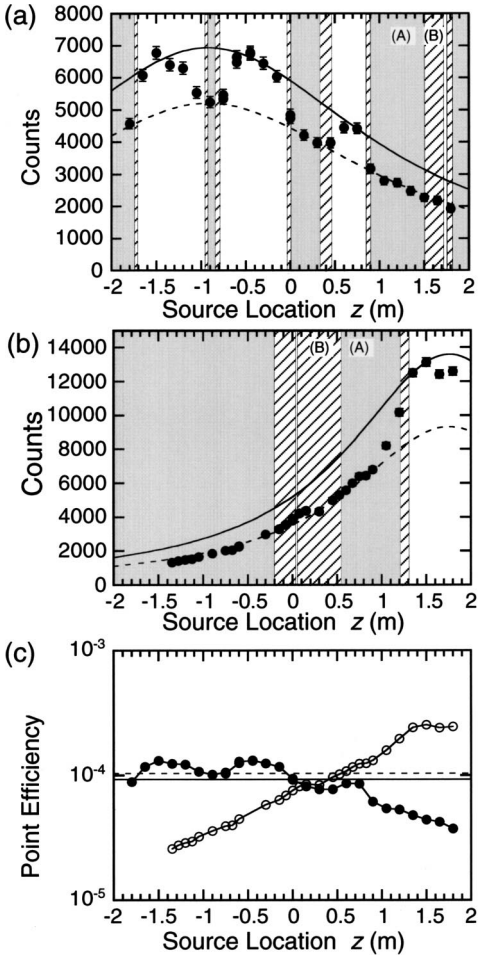

FIG. 3. Total counts obtained from the ^{3}He detectors (a) ^{3}He-1 and (b) ^{3}He-2 for a dwelling time of 576 s as a function of a ^{252}Cf source location on the z-axis inside the vacuum vessel. The hatching areas labeled (A) show the source locations, where the lines of sight of the ^{3}He detector cross the locations of the GAMMA 10 magnetic pancake coils and the coil supporting steel structures. The hatched area (B) represents the source locations, where a steel casing jacket covering over a magnetic coil alone crosses the lines of sight. An oscillatory behavior of the count variation in particular for ^{3}He-1 indicates the influence of the existence of the coils and the various coil supporting structures along the lines of sight of the detector. Most of the data points fit well to the curves proportional to the inverse of the source-detector distance squared, $1/d^2$ (the solid and the dashed curves). (c) The averaged point-detection efficiencies of the present detectors plotted by the solid line (^{3}He-1:9.3×10^{-5}) and the dashed line (^{3}He-2:1.0×10^{-4}) range about two orders-of-magnitude higher than that of the previous BF_3 neutron-monitoring system in GAMMA 10.

stainless-steel coil-casing jacket in the line of sight of ^{3}He-1. It is noted that the cooling water for the magnetic coils is filled during the calibration experiments so as to maintain the same conditions as those in the usual GAMMA 10 experiments. Some data points have unexpected signal degradations from the existence of such coil structures alone. It is, however, reasonably understood when one takes account of the influences of the existence of other structures including stainless-steel supporting legs for the coils.

To check the effect of the neutron-source transferring ''rail system'' on the neutron-detection counts, the neutron source is fixed at the central position ($z=0$) by the use of only a thin steel wire hanging from the topside of the vacuum vessel wall after the calibration experiments when

the whole source transfer system is removed. The difference observed between the cases with and without the transfer system is less than 0.5%.

For a scan of the neutron-source location in the z direction, the neutron detection efficiencies vary as a function of z because of the changes in the geometrical distance d from the detector to the source locations and the variation in the above-described effects from neutron scattering structures as a function of z. In general, it is anticipated that the neutron counts should have the $1/d^2$ dependence when no structural effects are taken into account. In fact, the solid curve in Fig. 3(a) representing the $1/d^2$ dependence fit well to the data points at $z=-1.65$, -1.50, -0.45, -0.30, -0.15, 0.60, and 0.75 m. On the other hand, the absolute values for the $1/d^2$ fitting are estimated to be 95% as compared to those in free space (i.e., without any obstacles in the lines of sight of the neutron detector). The difference is interpreted in terms of the existence of the 8-mm-thick GAMMA 10 vacuum vessel in the lines of sight. The dashed curve in Fig. 3(a) represents another $1/d^2$ fitting to the data points at $z=-1.80$, 0.15, 0.30, 0.45, as well as from $z=0.90$ to 1.80 m. The good fitting property of this dashed curve shows the dominant function is still the $1/d^2$ dependence even under the influences of the existence of the coils and structural materials in the line of sight of the detector.

Figure 3(b) shows the similar plots to those in Fig. 3(a) for ^{3}He-2. Most of the data points again fit to the $1/d^2$ dashed curve. The difference between Figs. 3(a) and 3(b) arises from the difference in the detector locations; that is, the location of ^{3}He-2 is quite near the GAMMA 10 device. The line of sight of the detector crosses the coil structural obstacles in $z<1.3$ m. For reference, the $1/d^2$ solid curve is also plotted in Fig. 3(b) for a fit to the data points of $z=1.35$ and 1.50 m, where no influence for the line of sight with the coil structural materials is anticipated.

B. Point efficiencies

Figure 3(c) shows the point efficiencies (i.e., the counts per unit neutron emission from a point source) of ^{3}He-1 (the filled circles) and ^{3}He-2 (the open circles) with respect to the source location. The averaged point efficiencies of ^{3}He-1 and ^{3}He-2 are 9.3×10^{-5} (the solid line) and 1.0×10^{-4} (the dashed line), respectively. A similar *in situ* calibration was made in 1994 for the previous neutron monitoring system with a BF_3 detector by the use of a ^{252}Cf source inside the GAMMA 10 vacuum vessel.[6] The averaged point efficiency of the previous BF_3 system can be estimated from the transmission factor (see Ref. 6), which gives the averaged point efficiency of 9.6×10^{-7}. Consequently, about two orders-of-magnitude higher neutron-detection efficiencies are achieved with the ^{3}He systems as compared to the previous BF_3 system.

The higher-detection efficiencies of the present ^{3}He systems enable us to analyze a neutron emissivity in a single plasma discharge alone. This contributes to the experiments for obtaining detailed plasma-parameter dependence by the use of limited available plasma discharges without any ambiguities from shot-to-shot irreproducible detailed properties of plasmas, since the use of the averaged neutron numbers over many plasma discharges gives various ambiguities.

The present neutron monitoring system plays an important role in tandem-mirror investigations to analyze the potential-confinement effects on improvements in plasma parameters as follows: The present typical hot-ion-mode experiments in GAMMA 10[2,6,7] with no direct auxiliary electron heatings provides a large difference between the hot-ion temperatures T_i ranging 5–10 keV and the bulk-electron temperatures T_e.[17–19] This, in turn, leads to a significant electron drag as the dominant energy-loss channel for the ICH-produced hot ions in the central cell. On the other hand, the scaling of T_e with the central-cell electron-confining potential (i.e., the thermal-barrier potential ϕ_b) is recently constructed on the basis of the generalized Pastukhov theory[11,12] and the electron energy-balance equation.[2,3] The results indicate that T_e increases with increasing the thermal transport-barrier depth ϕ_b. Such effectiveness of the potential improving the electron-energy confinement may contribute to ion heating by reducing the dominant energy loss term for hot ions. The reduction in the hot-ion energy loss, giving the T_i increase, may be followed by the improvement of the fusion reaction rate in D-D fusion experiments in GAMMA 10. This scenario for controlling the D-D fusion-produced neutrons or the fusion-reaction rate due to the thermal-barrier-potential control will be carried out by the use of the present calibrated ^{3}He detectors.

ACKNOWLEDGMENTS

The authors would like to acknowledge the members of the GAMMA 10 Group for their collaboration during the present international fusion cooperating research. This work was partially supported by a Grant-in-Aid for Scientific Research from the Ministry of Education, Culture, Sports, Science and Technology of Japan.

[1] T. Cho *et al.*, Phys. Rev. A **45**, 2532 (1992).
[2] T. Cho *et al.*, Phys. Rev. Lett. **86**, 4310 (2001).
[3] T. Cho *et al.*, Nucl. Fusion **41**, 1164 (2001).
[4] T. Cho *et al.*, Trans. Fusion Tech. **39**, 33 (2001).
[5] T. Cho *et al.*, Phys. Rev. Lett. **64**, 1373 (1990).
[6] Y. Kiwamoto *et al.*, Phys. Plasmas **3**, 578 (1996).
[7] K. Yatsu *et al.*, Nucl. Fusion **39**, 1707 (1999).
[8] M. Ichimura *et al.*, Nucl. Fusion **39**, 1995 (1999).
[9] S. Miyoshi *et al.*, Fiz. Plazmy **23**, 781 (1997) [Plasma Phys. Rep. **23**, 723 (1997)].
[10] R. H. Cohen *et al.*, Phys. Fluids **26**, 2774 (1983).
[11] V. P. Pastukhov, Nucl. Fusion **14**, 3 (1974).
[12] R. H. Cohen *et al.*, Nucl. Fusion **18**, 1229 (1978); R. H. Cohen, *ibid.* **19**, 1295 (1979); **19**, 1693 (1979).
[13] T. Nishitani *et al.*, Rev. Sci. Instrum. **63**, 5270 (1992).
[14] A. C. England *et al.*, PPPL-TM-400 (1993).
[15] G. F. Knoll, *Radiation Detection and Measurement*, 3rd ed. (Wiley, New York, 2000).
[16] S. Shalev *et al.*, Nucl. Instrum. Methods **71**, 292 (1969).
[17] J. Kohagura *et al.*, Rev. Sci. Instrum. **66**, 2317 (1995).
[18] J. Kohagura *et al.*, Rev. Sci. Instrum. **70**, 633 (1999).
[19] J. Kohagura *et al.*, Phys. Rev. E **56**, 5884 (1997).